HHS Public Access

Author manuscript

Mucosal Immunol. Author manuscript; available in PMC 2018 May 31.

Published in final edited form as:

Mucosal Immunol. 2018 May ; 11(3): 909–920. doi:10.1038/mi.2017.96.

Detection of HIV-1-Specific Gastrointestinal Tissue Resident CD8+ T-cells in Chronic Infection

Brenna E. Kiniry[1], **Shengbin Li**[2], **Anupama Ganesh**[1], **Peter W. Hunt**[3], **Ma Somsouk**[4], **Pamela J. Skinner**[2], **Steven G. Deeks**[3], and **Barbara L. Shacklett**[*,1,5]

[1]Department of Medical Microbiology and Immunology, School of Medicine, University of California, Davis, CA USA

[2]Department of Veterinary and Biomedical Sciences, University of Minnesota, St. Paul, MN

[3]Positive Health Program, Department of Medicine, San Francisco General Hospital, San Francisco, CA USA

[4]Division of Gastroenterology, Dept. of Medicine, San Francisco General Hospital, San Francisco, CA USA

[5]Division of Infectious Diseases, Dept. of Medicine, School of Medicine, University of California, Davis, CA USA

Abstract

Tissue-resident memory (T_{RM}) $CD8^+$ T-cells are non-recirculating, long-lived cells housed in tissues that can confer protection against mucosal pathogens. HIV-1 is a mucosal pathogen and the gastrointestinal tract is an important site of viral pathogenesis and transmission. Thus, $CD8^+$ T_{RM} cells may be an important effector subset for controlling HIV-1 in mucosal tissues. This study sought to determine the abundance, phenotype, and functionality of $CD8^+$ T_{RM} cells in the context of chronic HIV-1 infection. We found that the majority of rectosigmoid $CD8^+$ T-cells were $CD69^+CD103^+S1PR1^-$ and T-$bet^{Low}Eomesodermin^{Neg}$, indicative of a tissue-residency phenotype similar to that described in murine models. HIV-1-specific $CD8^+$ T_{RM} responses appeared strongest in individuals naturally controlling HIV-1 infection. Two $CD8^+$ T_{RM} subsets, distinguished by CD103 expression intensity, were identified. $CD103^{Low}$ $CD8^+$ T_{RM} primarily displayed a transitional memory phenotype and contained HIV-1-specific cells and cells expressing high levels of Eomesodermin, whereas $CD103^{High}$ $CD8^+$ T_{RM} primarily displayed an

*Name and Address for Correspondence: Barbara L. Shacklett, PhD, Dept. of Medical Microbiology and Immunology, UC Davis School of Medicine, 3146 Tupper Hall, Davis CA 95616, Tel: 530 752 6785; Fax: 530 752 8692, blshacklett@ucdavis.edu.

The authors declare no conflicts of interest that could be perceived to bias this work.

Supplementary Material is linked to the online version of the paper at http://www.nature.com/mi

AUTHOR CONTRIBUTIONS

Project concept and direction: BLS with consultation from PS, PWH and SGD. Characterization of participant cohort and procurement of clinical samples: MS, PWH, SGD. Laboratory assays: BEK (flow cytometry) with assistance from AG; SL (in situ tetramer staining). Data analysis: BEK, SL, PS, BLS. Manuscript writing and editing: BEK, BLS. All authors read and approved the manuscript.

DISCLOSURE

The authors report no conflicts of interest that could be perceived to bias this work.

effector memory phenotype and were Eomesodermin^{Neg}. These findings suggest a large fraction of CD8$^+$ T-cells housed in the human rectosigmoid mucosa are tissue-resident and that T_{RM} contribute to the anti-HIV-1 immune response. Further exploration of CD8$^+$ T_{RM} will inform development of anti-HIV-1 immune-based therapies and vaccines targeted to the mucosa.

INTRODUCTION

The gastrointestinal mucosa is an important site of HIV-1 pathogenesis, as it serves both as a portal of entry and site of HIV-1 persistence throughout chronic infection[1]. Accordingly, immune-based strategies to prevent and/or eradicate HIV-1 infection will likely require durable and robust HIV-1-specific immune responses in the rectosigmoid mucosa and other vulnerable tissues[2, 3, 4, 5]. Characterized as long-lived, non-recirculating effector memory T-cells localized to tissues including the gastrointestinal tract, tissue-resident memory T-cells (T_{RM}) represent a potential immunotherapeutic target for combating mucosal pathogens such as HIV-1[6, 7, 8, 9].

First described in the murine model, T_{RM} are thought to develop from killer cell lectin like receptor G1 (KLRG1)-negative precursor effector T-cells following migration into peripheral tissues[10]. Here, exposure to tissue-specific cytokine mixtures involving TGF-β drives expression of early activation marker CD69 and integrin αE(CD103)β_7, which promote tissue accumulation and retention and are considered hallmarks of the T_{RM} phenotype[6, 11, 12, 13, 14]. Interestingly, although T-box transcription factors Eomesodermin and T-bet regulate CD8$^+$ T-cell development and effector function, a feature of CD103$^+$ CD8$^+$ T_{RM} conserved across models of infection is strong down-regulation of Eomesodermin (Eomes)[12, 15]. Recently, using a murine Herpes simplex virus-1 model, skin CD8$^+$ T_{RM} were shown to display low T-bet and negligible Eomes expression[16]. Unlike circulating effector memory CD8$^+$ T-cells, T_{RM} in the gastrointestinal tract appear to be maintained independently of cognate antigen for long periods[7, 11, 17, 18]. Positioned at sites of pathogen exposure, T_{RM} initiate rapid and robust defenses upon reinfection, notably cytokine production, mobilizing both innate and adaptive arms of the immune system[10]. Studies of lung, skin, genital mucosa, and small intestine have all demonstrated the protective capacity of T_{RM} against a range of pathogens after secondary infection and during reactivation of latent viral infection[17, 19, 20, 21, 22, 23, 24]. Together, these data suggest T_{RM} may be beneficial in controlling HIV-1 infection in peripheral, non-lymphoid tissues like the gastrointestinal mucosa.

Although the protective attributes of T_{RM} have been characterized extensively in murine models, a knowledge gap exists regarding their role in HIV-1 infection. Previous characterization of mucosal CD8$^+$ T-cells in chronic HIV-1 infection revealed them to be phenotypically and functionally different from CD8$^+$ T-cells circulating in blood. Rectosigmoid CD8$^+$ T-cells displayed weak perforin-mediated cytotoxicity and diminished expression of T-bet and Eomesodermin compared to their blood counterparts[25, 26, 27]. Rather, rectosigmoid CD8$^+$ T-cells were primarily T-bet^{Low}Eomesodermin^{Neg} and displayed robust cytokine/chemokine polyfunctionality characteristic of T_{RM}. Strong polyfunctional HIV-1-specific CD8$^+$ T-cell responses in rectosigmoid mucosa have been identified as a

correlate of immune control as they are particularly robust in individuals who naturally control HIV-1 (i.e. "controllers")[26]. Whether these observations reflect an abundance of canonical 'tissue-resident' $CD8^+$ T-cells in human gastrointestinal mucosa and participation of T_{RM} in controlling HIV-1-infection is unknown.

The goal of this study was to determine whether gastrointestinal HIV-1-specific $CD8^+$ T-cells in chronically HIV-1-infected and healthy participants share the characteristics of tissue resident T-cells as described in murine models of infectious disease, and to better understand the implications of this understudied population for HIV-1 pathogenesis, immune control, and vaccine design.

RESULTS

Most $CD8^+$ T-cells in human rectosigmoid mucosa display a tissue-resident phenotype

T_{RM} can be distinguished from recirculating populations via expression of tissue-specific markers and the absence of recirculation markers[8, 19]. Co-expression of CD69 and αE integrin (CD103) in the absence of sphingosine-1-phosphate receptor (S1PR1) and C–C motif chemokine receptor 7 (CCR7) are commonly used to identify tissue-resident $CD8^+$ T-cells in a range of tissues[6, 13, 14, 28]. To determine whether this strategy also identifies tissue-resident $CD8^+$ T-cells in human rectosigmoid mucosa, we used flow cytometry to analyze cells for expression of CD103, CD69, and S1PR1 in chronically HIV-1-infected and seronegative participants.

Irrespective of HIV-1 disease status, large fractions of rectosigmoid $CD8^+$ T-cells were $CD103^+CD69^+S1PR1^-$; in contrast, this subset was negligible in blood (Figure 1a–b). In tissues, effector memory $CD8^+$ T-cells often display a tissue-residency phenotype [6, 28, 29, 30, 31]; however, the extent to which other memory subsets display such a phenotype is not known. We next analyzed expression of CD103, CD69, and S1PR1 within rectosigmoid $CD8^+$ T-cell memory subsets in HIV-1^+ and seronegative participants. Memory subsets were defined as follows: naïve ($CD45RO^-CD27^+CCR7^+$), central memory ($CD45RO^+CD27^+CCR7^+$), transitional memory ($CD45RO^+CD27^+CCR7^-$), effector memory ($CD45RO^+CD27^-CCR7^-$), and effector ($CD45RO^-CD27^-CCR7^-$)(Supplementary Figure 1a–b)[32, 33]. Although the abundance of naïve (T_{naive}) and central memory (T_{CM}) $CD8^+$ T-cells in mucosa was low compared to effector (T_{EFF}) and effector memory (T_{EM}) T-cells, all memory subsets contained some $CD103^+CD69^+S1PR1^-$ $CD8^+$ T-cells, the proportion of which increased with memory differentiation. Only a small fraction of T_{naive} and T_{CM} $CD8^+$ T-cells were $CD103^+CD69^+S1PR1^-$ (medians 2.16% and 19.5%, respectively); in contrast, large proportions of T_{EFF} and T_{EM} were $CD103^+CD69^+S1PR1^-$ (medians 64.7% and 74.9%, respectively)(Figure 1c–d). We also observed CD103 expressed at high and low median fluorescence intensities (MFI) on rectosigmoid $CD8^+$ T-cells. While the majority of rectosigmoid tissue-resident $CD8^+$ T-cells were $CD103^{High}$, a small percentage was $CD103^{Low}$; this percentage varied with memory differentiation. The proportion of $CD103^{Low}$ $CD69^+S1PR1^-$ putative tissue-resident $CD8^+$ T-cells was highest among T_{TM} and T_{CM}, and lowest among T_{naive} (Figure 1c–e).

CD103 binds β7 to form the heterodimeric integrin αEβ7, which interacts with E-cadherin on epithelial cells, facilitating accumulation of tissue-resident T-cells in close proximity to the epithelium[34, 35, 36]. We used immunohistochemistry and quantitative image analysis to confirm the distribution of $CD103^{Neg}$, $CD103^{Low}$, and $CD103^{High}$ $CD8^+$ T cells. Cells were quantified in three anatomical compartments within rectosigmoid mucosa: intraepithelial lymphocytes (IE), lamina propria (LP), and areas bordering (B) the IE and LP (Supplementary Figure 2a). $CD103^{Neg}$ $CD8^+$ T cells were located primarily in the LP, in contrast, greater than 60% of $CD103^{High}$ $CD8^+$ T cells and approximately 50% of $CD103^{Low}$ $CD8^+$ T cells were intraepithelial (Supplementary Figure 2a–c). These findings corroborate previous observations concerning the localization of CD103-expressing $CD8^+$ T-cells in human intestine[34, 35] and reveal that a large proportion of rectosigmoid $CD8^+$ T-cells resemble tissue-resident cells described previously. In human rectosigmoid mucosa, this population is composed mainly of $CD103^{High}$ effector and effector memory cells.

$CD103^{High}$ and $CD103^{Low}$ tissue-resident $CD8^+$ T-cells differ in abundance across HIV-1 disease status, association with rectosigmoid $CD4^+$ T-cells, and expression of memory markers

Disruption of the gut epithelial barrier and dramatic depletion of gut $CD4^+$ T-cells are hallmarks of HIV-1 infection[5, 37]. $CD4^+$ T-cells have been shown to aid development of lung $CD103^{High}$ $CD8^+$ T_{RM} during influenza infection[10, 38]. Accordingly, we hypothesized that the abundance of $CD103^{High}$ tissue-resident $CD8^+$ T-cells might be lower in chronically HIV-1-infected compared to seronegative participants. To test this, we evaluated expression of tissue-resident markers on unstimulated rectosigmoid $CD8^+$ T-cells in the following groups: HIV-1^+ controllers (C); HIV-1^+ viremic individuals not on antiretroviral therapy (V); HIV-1^+ individuals on antiretroviral therapy (Tx); and seronegative controls (SN) (Table 1). As $CD8^+$ T-cells displaying a tissue-resident phenotype were primarily observed in effector memory and effector subsets, we investigated both $CD45RO^+$ and $CD45RO^{Neg}$ populations; referring to $CD45RO^+$ $CD103^+CD69^+S1PR1^-$ cells as tissue-resident memory cells (T_{RM}) and $CD45RO^{Neg}$ $CD103^+CD69^+S1PR1^-$ cells as tissue-resident effector cells, abbreviated rT_{EFF}.

As expected, HIV-1^+ participants not on antiretroviral therapy (ART) displayed lower proportions of $CD103^{High}$ $CD8^+$ T_{RM} and rT_{EFF} compared to HIV-1^+ participants on ART and seronegatives, reaching statistical significance for ART-treated compared to controllers and viremic untreated individuals for T_{RM}, and between viremic untreated and seronegatives for rT_{EFF} (Figure 2a–b). No differences between subject groups were observed in the proportions of $CD103^{Low}$ T_{RM} and rT_{EFF} (data not shown). When all participant groups were combined, a strong positive correlation was observed between the percentage of rectosigmoid $CD4^+$ T-cells and that of $CD103^{High}$ but not $CD103^{Low}$ T_{RM} (Figure 2c). A similar correlation was seen when all HIV-1^+ participants were considered together ($P=0.0048$, $R^2=0.44$); however, when each subgroup (including seronegatives) was examined individually, no significant differences or trends were observed (not shown). No correlations were observed between rectosigmoid $CD4^+$ T-cells and the percentages of $CD103^{High}$ or $CD103^{Low}$ rT_{EFF} cells (Supplementary Figure 3a).

CD103^{High} and CD103^{Low} tissue-resident CD8^{+} T-cells also differed in memory phenotype. The majority of CD103^{High} T_{RM} displayed an effector memory phenotype (T_{EM} median 67.7%, T_{TM} median 32.2%, T_{CM} median 0.225%); in contrast, CD103^{Low} T_{RM} cells mainly displayed a transitional memory phenotype characterized by expression of CD27 (T_{TM} median 77.6%, T_{EM} median 20.6%, T_{CM} median 1.05%)(Figure 2d–e). Among rT_{EFF}, CD103^{High} cells primarily displayed the canonical effector phenotype (CD45RO^{-}CD27^{-}CCR7^{-}, median 73.5%), whereas a substantial fraction of CD103^{Low} rT_{EFF} expressed CD27 (CD45RO^{-}CD27^{+}CCR7^{-} median 55.4%) (Supplementary Figure 3b–c). Collectively, these data reveal lower proportions of highly differentiated T_{EM}/T_{EFF} CD103^{High} tissue-resident CD8^{+} T-cells in HIV-1^{+} individuals not on ART compared to ART-treated and seronegative groups, and a strong association between CD103^{High} CD8^{+} T_{RM} cells and rectosigmoid CD4^{+} T-cells.

HIV-1 gag-specific tissue-resident CD8^{+} T-cell responses originate from CD103^{Low} cells and appear strongest in controllers

Although tissue-resident T-cells represent a potential immunotherapeutic target for HIV-1 eradication, little is known about the contribution these cells to the HIV-1-specific immune response during chronic infection. This and previous work have revealed the presence of HIV-1 Gag-specific, MHC class I tetramer-binding CD8^{+} T-cells expressing αEβ7 in human rectosigmoid mucosa[30] (Supplementary Figure 2d), and studies in rhesus macaques demonstrated vaccine-inducible long-lasting mucosal T-cell responses, suggesting T_{RM} contribute to the HIV-1-specific immune response[18, 39]. We investigated Gag-specific tissue-resident CD8^{+} T-cell responses and their contribution to the total rectosigmoid Gag-specific CD8^{+} T-cell response across HIV-1-disease status using an *ex vivo* 6h stimulation assay followed by intracellular staining for effector molecules.

Degranulation (CD107a) and cytokine production in response to Gag-peptide stimulation were detected in rectosigmoid CD8^{+} T_{RM} and rT_{EFF}, with T_{RM} displaying significantly higher percentages of Gag and SEB-responding cells compared to rT_{EFF} (Figure 3a–b). Both controllers and viremic participants not on ART displayed significantly greater total and polyfunctional Gag-specific tissue-resident CD8^{+} T-cell responses compared to ART-treated participants (Figure 3c–e). This parallels earlier cross-sectional studies, in which we found low percentages of total and polyfunctional Gag-specific T-cells in mucosal tissues of participants on ART, particularly those with viral suppression[25, 26, 27]. Although the total HIV-1 Gag-specific response did not differ significantly in magnitude between controllers and viremic untreated participants, the highest median polyfunctional responses (3- and 4-function) were detected in controllers (Figure 3d–e). This was true for both T_{RM} (Figure 3d) and rT_{EFF} (Figure 3e). The strongest polyfunctional responses elicited by both T_{RM} and rT_{EFF} involved CD107a, MIP-1β, and IFN-γ, with all notable polyfunctional responses involving CD107a (Figure 3d–e). With the exception of IL-2-producing cells, Gag-responding CD8^{+} T_{RM} were primarily CD103^{Low}, reaching statistical significance for CD107a- and IFN-γ-producing T_{RM}; in contrast, SEB-responding T_{RM} were primarily CD103^{High} (Supplementary Figure 4a–b). Similar trends were observed for Gag-responding CD8^{+} rT_{EFF} (Supplementary Figure 4c).

Previous work has demonstrated robust polyfunctional HIV-1-specific $CD8^+$ T-cell responses in rectosigmoid mucosa of controllers[26]; however, it is unknown whether these responses originate from resident and/or circulating populations. To understand the extent to which tissue-resident cells contribute to the total HIV-1 Gag-specific $CD8^+$ T-cell response in rectosigmoid mucosa, we analyzed expression of CD69, CD103, and S1PR1 on Gag-specific polyfunctional $CD8^+$ T-cells, focusing on the $CD107a^+MIP\text{-}1\beta^+IFN\text{-}\gamma^+$ ($7^+M^+F^+$) response as it had the highest median frequency (Supplementary Figure 5). Rectosigmoid Gag-specific $7^+M^+F^+$ $CD8^+$ T-cells displayed three main patterns: the canonical tissue-resident phenotype ($CD103^+CD69^+S1PR1^-$), CD69 single positive ($CD103^-CD69^+S1PR1^-$), and absence of all three markers ($CD103^-CD69^-S1PR1^-$); the proportions differed between viremic individuals not on ART and controllers. In viremic individuals, rectosigmoid Gag-specific $7^+M^+F^+$ $CD8^+$ T-cells were primarily tissue-resident (median 35.9%) or CD69 single positive (median 38.7%) with a smaller fraction lacking all three markers (median 11.6%). In controllers, the majority of $7^+M^+F^+$ $CD8^+$ T-cells were CD69 single positive (median 52.2%) with much smaller proportions exhibiting tissue-residency (median 16.0%) or absence of all three markers (median 16.7%)(Supplementary Figure 5a–c). These trends were conserved across all polyfunctional responses (data not shown). The results presented here, in conjunction with previous work, demonstrate that HIV-1-specific tissue-resident $CD8^+$ T-cells are present in rectosigmoid mucosa and capable of polyfunctional responses. In the context of chronic HIV-1 infection, Gag-specific tissue-resident $CD8^+$ T-cells appear to be mainly $CD103^{Low}$. Notably, although tissue-resident Gag-specific $CD8^+$ T-cell responses appeared strongest in controllers, the tissue-resident population constituted a smaller proportion of the total rectosigmoid Gag-specific $CD8^+$ T-cell response in controllers compared to viremic participants not on ART.

Eomesodermin expression in tissue-resident $CD8^+$ T-cells is associated with low CD103 fluorescence intensity and is greatest in $HIV\text{-}1^+$ participants not on ART

Previous work demonstrated that although human rectosigmoid $CD8^+$ T-cells typically had a $T\text{-}bet^{Low}Eomesodermin^{Neg}$ phenotype characteristic of T_{RM}, $HIV\text{-}1^+$ individuals not on ART displayed greater Eomes expression compared to ART-treated and healthy participants[27]. Whether this reflects up-regulation of Eomes by tissue-resident $CD8^+$ T-cells or an influx of $Eomes^{High}$ $CD8^+$ T-cells from circulation is unknown. To elucidate the origin of $Eomes^{High}$ $CD8^+$ T-cells in rectosigmoid mucosa and understand modulations in T-bet and Eomes expression during chronic HIV-1 infection, we used flow cytometry to detect intracellular T-bet and Eomes, in conjunction with tissue-resident markers, in unstimulated rectosigmoid $CD8^+$ T-cells from $HIV\text{-}1^+$ individuals and healthy controls (Figure 4; Supplementary Figure 6).

Rectosigmoid $Eomes^{High}$ $CD8^+$ T-cells were primarily single positive for CD69 ($CD103^-CD69^+S1PR1^-$ median 47.4%); however, a notable fraction displayed the canonical tissue-resident phenotype ($CD103^+CD69^+S1PR1^-$, median 26.6%)(Supplementary Figure 6b–c). To determine whether high Eomes expression observed in the $CD103^+CD69^+S1PR1^-$ subset was associated with chronic HIV-1 infection, we compared Eomes expression in $CD8^+$ T_{RM} and rT_{EFF} cells across HIV-1 disease status (Figure 4a–b). Similar to the total rectosigmoid $CD8^+$ T-cell population, tissue-resident $CD8^+$ T-cells were primarily T-

bet$^{Low/Neg}$Eomes^{Neg}; however, HIV-1^{+} participants not on ART had higher percentages of Eomes^{High} tissue-resident CD8^{+} T-cells compared to ART-treated and seronegative participants. Unlike Eomes, no differences in T-bet expression were observed between groups (Figure 4). Within the T_{RM} subset, viremic individuals not on ART displayed the highest median frequency of Eomes^{High} cells; however within rT_{EFF}, only HIV-1 controllers displayed significantly greater Eomes expression compared to ART-treated and seronegative groups (Figure 4a–b, Supplementary Figure 7a). The majority of Eomes^{High} tissue-resident CD8^{+} T-cells were CD103^{Low}; in contrast, Eomes^{Neg} cells were primarily CD103^{High} (Figure 4c–d, Supplementary Figure 7b). Together, these data demonstrate that rectosigmoid tissue-resident CD8^{+} T-cells are primarily CD103^{High} T-bet$^{Low/Neg}$Eomes^{Neg}; however, in untreated HIV-1 infection, a substantial population of CD103^{Low} Eomes^{High} tissue-resident CD8^{+} T-cells emerges.

DISCUSSION

Several studies have demonstrated the disparity in phenotype and function between CD8^{+} T-cells isolated from gastrointestinal mucosa and peripheral blood[25, 26, 27]. As the gut is an important site of HIV-1 pathogenesis, these findings highlight the importance of understanding the distinct properties of mucosal immune responses to HIV-1[5]. With the discovery of tissue-resident CD8^{+} T-cells, numerous studies have eloquently described the tissue-specific mechanisms that shape the tissue-resident population as well as the capacity of tissue-resident CD8^{+} T-cells to protect the host against mucosal pathogens[9, 10]. Missing from this body of knowledge, however, is an understanding of the role of tissue-resident CD8^{+} T-cells in fighting HIV-1 infection in the gastrointestinal mucosa, a site of viral transmission and pathogenesis[5, 37]. Thus, the aim of this study was to investigate the abundance of tissue-resident CD8^{+} T-cells in human rectosigmoid mucosa and the contribution of tissue-resident CD8^{+} T-cells to the HIV-1-specific immune response during chronic infection.

The majority of CD8^{+} T-cells in human rectosigmoid mucosa were CD103^{+}CD69^{+}S1PR1^{-}, with a T-bet^{Low}Eomes^{Neg} transcriptional profile reminiscent of tissue-resident CD8^{+} T-cells described in the literature[10]. This subset was negligible in blood, further evidence of the tissue-resident nature of these cells. As effector memory cells predominate in mucosal tissues and play an important role in secondary immune responses, most tissue-resident work has focused on memory T-cells[31]. Indeed, the majority of rectosigmoid effector memory CD8^{+} T-cells were CD103^{+}CD69^{+}S1PR1^{-}, expanding on previous work demonstrating an abundance of effector memory CD8^{+} T-cells expressing CD69 and CD103 in jejunum, ileum, and colon of human cadavers[28, 31]. Additionally, the majority of effector CD8^{+} T-cells in rectosigmoid mucosa also displayed tissue-residency. Although the origin of this putative resident effector population, termed rT_{EFF}, could not be definitively determined, one interpretation is that rT_{EFF} are memory precursor effector cells (MPEC) transitioning into T_{RM}. In murine skin and intestine, T_{RM} develop from KRLG1^{Neg} MPECs[12, 36]. In an oral *Listeria monocytogenes* murine model, intestinal intraepithelial KLRG1^{Neg} MPECs were CD103^{+}CD69^{+} and formed rapidly compared to spleen or lung MPECs in a TGF-β-dependent manner[36]. Interestingly, we observed that although expression of KLRG1 was relatively low on rectosigmoid rT_{EFF} and T_{RM} compared to blood

$CD8^+$ T-cells, rT_{EFF} displayed significantly lower expression of KLRG1 compared to T_{RM} cells (these authors, unpublished data). Alternatively, rT_{EFF} may represent a mature tissue-resident population distinct from T_{RM}. Longitudinal studies designed to track the appearance and longevity of pathogen-specific rT_{EFF} may help elucidate the origin and role of rT_{EFF} in mucosal immunity.

Previous studies reported robust polyfunctional Gag-specific $CD8^+$ T-cells in rectosigmoid mucosa of controllers, identifying these cells as a possible correlate of immune control[25, 26, 40]. However, it remains unclear whether recent emigrants from blood or resident populations mediate these responses. We detected Gag-specific responses in both T_{RM} and rT_{EFF} populations, demonstrating that tissue-resident T-cells contribute to the HIV-1-specific immune response. Although this study did not have the statistical power to discern differences between controllers and viremic untreated individuals, the strongest median polyfunctional T_{RM} and rT_{EFF} responses were detected in controllers, suggesting tissue-resident $CD8^+$ T-cells might play a role in controlling HIV-1 in rectosigmoid mucosa. Paradoxically, although controllers displayed the highest median percentages of polyfunctional Gag-specific tissue-resident $CD8^+$ T-cell responses, these responses constituted a smaller proportion of the total rectosigmoid Gag-specific $CD8^+$ T-cell response in controllers compared to viremic participants not on ART. Instead, in controllers, the majority of rectosigmoid Gag-specific polyfunctional $CD8^+$ T-cells were single positive for CD69. CD69 is an early activation marker up-regulated on tissue-resident precursor cells after entering the tissue. Expression of CD69 occurs early in tissue-resident development, preceding CD103 expression, and aids in tissue-retention by repressing expression of the tissue egress receptor S1PR1[12, 13, 14, 41]. Tissue-resident $CD8^+$ T-cells have been shown to initiate immune responses, mediated through cytokine and chemokine secretion, leading to recruitment of circulating immune cells to the site of infection[22, 23]. Accordingly, one interpretation of these data is that individuals with more robust Gag-specific tissue-resident $CD8^+$ T-cell responses (i.e., HIV-1 controllers) might in turn experience greater recruitment of HIV-1-specific $CD8^+$ T-cells from circulation compared to individuals with weaker $CD8^+$ tissue-resident responses. This enhanced recruitment of cells lacking the tissue-resident phenotype would dilute the proportion of Gag-specific cells in rectosigmoid mucosa with a tissue-resident phenotype, consistent with our observations. Clearly, further studies, likely involving nonhuman primate models, will be required to fully elucidate the role of tissue-resident $CD8^+$ T-cells in the total mucosal anti-HIV-1 immune response.

Within both T_{RM} and rT_{EFF} populations, we observed two subsets of tissue-resident $CD8^+$ T-cells that could be differentiated by CD103 fluorescence intensity. The $CD103^{High}$ subset resembled canonical tissue-resident $CD8^+$ T-cells, consisting mainly of T_{EM}/T_{EFF} cells with a T-$bet^{Low}Eomes^{Neg}$ profile. $CD103^{High}$ cells were enriched in epithelia and revealed a strong positive correlation with the percentage of rectosigmoid $CD4^+$ T-cells. In contrast, the $CD103^{Low}$ subset was mainly composed of less-differentiated $CD8^+$ T-cells expressing CD27, and was more abundant in lamina propria compared to $CD103^{High}$ cells. HIV-1^+ individuals not on ART had lower percentages of $CD103^{High}$ but higher percentages of $Eomes^{High}$ tissue-resident $CD8^+$ T-cells compared to ART-treated participants and seronegative controls. Interestingly, both Gag-specific and $Eomes^{High}$ tissue-resident $CD8^+$ T-cells were primarily $CD103^{Low}$. Collectively, these observations reveal heterogeneity in

the tissue-resident $CD8^+$ T-cell population that may be exacerbated during chronic untreated HIV-1 infection.

Three main interpretations, not mutually exclusive, emerged to explain the observed HIV-1-associated alterations in the tissue-resident $CD8^+$ T-cell population. First, gut epithelial cells express E-cadherin and are a constitutive source of TGF-β, a prominent driver of tissue-resident development[6, 7, 12, 16, 36, 42, 43]. Certain subsets of $CD4^+$ T-cells also produce TGF-β and $CD4^+$ T-cells have been shown to aid development of T_{RM} in the lung[38, 44]. Accordingly, loss of epithelial barrier function and/or $CD4^+$ T-cells during HIV-1 infection may result in a reduction of gut TGF-β and E-cadherin, ultimately leading to a reduction in an accumulation and/or development of $CD103^{High}$ tissue-resident $CD8^+$ T-cells. Second, chronic antigen exposure can affect CD103 expression. In murine lymphocytic choriomeningitis virus (LCMV) infection, chronic *in vivo* exposure to antigen in combination with TGF-β reduced CD103 expression on antigen-specific $CD8^+$ T-cells, leading the authors to propose CD103 as a marker for resting versus recently stimulated T_{RM}[7]. Consistent with this finding, we observed Gag-specific tissue-resident $CD8^+$ T-cells to be primarily $CD103^{Low}$ whereas tissue-resident $CD8^+$ T-cells responding to SEB were primarily $CD103^{High}$. It seems unlikely that the significant reduction in the percentage of $CD103^{High}$ tissue-resident $CD8^+$ T-cells observed in HIV-1^+ individuals not on ART would be due solely to CD103 down-regulation on HIV-1-specific cells. However, the pool of rectosigmoid tissue-resident $CD8^+$ T-cells undergoing activation-induced CD103 down-regulation might be broadened in individuals not on ART due to 'bystander' activation as a result of HIV-1-associated inflammation[37]. Third, the HIV-1-associated inflammatory state in individuals not on ART might lead to greater recruitment of $CD8^+$ T-cells from circulation. An influx of blood $CD8^+$ T-cells into rectosigmoid mucosa would reduce the proportion of $CD103^{High}$ cells in the total rectosigmoid $CD8^+$ T-cell population and increase proportions of $CD103^{Low/Neg}$ cells as recent immigrants mature into $CD103^{High}$ tissue-residents. In support of this interpretation, a large fraction of $CD103^{Low}$ tissue-resident $CD8^+$ T-cells displayed a less differentiated memory phenotype characterized by CD27 expression.

Again, these interpretations are likely not mutually exclusive. The $CD103^{Low}$ tissue-resident $CD8^+$ T-cell subset may be heterogeneous, composed both of recent immigrants developing into tissue-resident $CD8^+$ T-cells and activated, mature tissue-resident $CD8^+$ T-cells. Interestingly, within the $CD103^{Low}$ subset, we observed heterogeneity in Eomes expression. Unlike $CD103^{High}$ cells, which displayed a homogenous T-$bet^{Low}Eomes^{Neg}$ phenotype, the $CD103^{Low}$ subset contained cells expressing high, low, or no Eomes. Notably, although $CD103^{Low}$ cells were primarily $Eomes^{Neg}$, $Eomes^{High}$ tissue-resident $CD8^+$ T-cells were almost exclusively $CD103^{Low}$. Murine skin and brain tissue-resident $CD8^+$ T-cells severely down-regulate Eomes; thus, detecting high Eomes expression within this population was surprising[12, 15, 16]. However, high Eomes expression has been associated with a 'terminally exhausted' phenotype when co-expressed with the inhibitory receptor programmed cell death-1 (PD-1)[45]. As the frequency of $Eomes^{High}$ tissue-resident $CD8^+$ T-cells was greatest in HIV-1^+ individuals not on ART, we surmised that the high Eomes expression in rectosigmoid tissue-resident $CD8^+$ T-cells likely represents activated and/or exhausted cells. The data presented here do not contradict previous findings, but rather suggest that Eomes

expression may vary during chronic infection and that tissue-resident $CD8^+$ T-cells may be susceptible to exhaustion.

To our knowledge, this is the first report examining the characteristics and functionality of tissue-resident $CD8^+$ T-cells in rectosigmoid mucosa during HIV-1 infection. As the gastrointestinal mucosa is an important site of HIV-1 transmission and pathogenesis[1], the long-lived tissue resident T-cell population can potentially be exploited in the development of vaccines and immunotherapies designed to prevent and/or eradicate HIV-1 infection. Recent successes in HIV-1 vaccine development have lent support to the concept that antigen-specific $CD8^+$ T-cells, positioned near the sites of mucosal viral entry, can play critical roles in preventing and/or clearing infection[4, 18, 39]. However, more work will be required to fully elucidate the pathways driving induction and maintenance of these populations, and to understand the relative contributions of both tissue-resident and recirculating memory T-cell subsets to host immunity.

METHODS

Participants and Sample Collection

HIV-1 positive and seronegative participants were enrolled through the SCOPE study at San Francisco General Hospital. Participants were categorized by plasma viral load (VL) and antiretroviral therapy (ART): Controllers (C) with VL consistently <2,000 copies/mL without ART; Viremic (V) subjects with VL ≥ 2,000 copies/mL without ART; ART treated (Tx) participants with VL < 40 copies/mL; and HIV-1 seronegatives (SN). Seronegative participants were healthy volunteers from whom samples were collected for research purposes only. Written informed consent for phlebotomy and rectosigmoid biopsy was obtained through protocols approved by the Committee on Human Subjects Research, University of California, San Francisco [Protocols #10-01218, 10-00263 and 10-01330]. Exclusion criteria included active sexually transmitted infections other than HIV-1; inflammatory bowel disease or other known inflammatory conditions affecting the gastrointestinal tract; colorectal cancer or other malignancies; and severe anemia or blood clotting disorders.

Twenty to 40 ml of blood was collected by sterile venipuncture into tubes containing EDTA. Twenty-four to 30 rectosigmoid biopsies were obtained by flexible sigmoidoscopy at 10–30cm from the anal verge[2]. Biopsies were immediately stored in R-15 [RPMI-1640 supplemented with fetal calf serum (15%), penicillin (100U/mL), streptomycin (100 mg/mL), and glutamine (2 mM)]. Samples were transported at room temperature to Davis, CA and processed immediately upon arrival.

Blood and Tissue Processing

Peripheral blood mononuclear cells (PBMCs) were isolated from blood using Ficoll-Paque™ (Pfizer-Pharmacia, New York, NY) and rested overnight in R-15 at 37°C, 5% CO_2. Rectosigmoid mononuclear cells were isolated from biopsies as described[46, 47]. Briefly, biopsies were washed in R-15 and subjected to shaking incubation in 25mg/mL Liberase® DL (Roche, Indianapolis, IN) at 37°C for 30 minutes, then passed through a 16-gauge blunt

end needle to mechanically disrupt tissue. Disrupted tissue was passed through a sterile 70μm cell strainer to collect cells. Undigested tissue was again incubated in Liberase and the process repeated until all tissue was digested. Isolated cells were washed three times in R-15 and rested overnight at 37°C, 5% CO_2 in R-15 with 200x Zozyn (Pfizer-Pharmacia).

Antibodies and Peptide Pools

The following monoclonal antibodies were used in flow cytometry: CD8 (SK1: APC-H7), CCR7 (3D12: PE-Cy7), CD69 (L78: PE), IFN-γ (B27: PE-Cy7), MIP-1β (D21-1351: PerCP-Cy5.5), from BD Biosciences (San Jose, CA); CD103 (Ber-ACT8: Ax488), TNF-α (MAb11: BV605), IL-2 (MQ1-17H12: BV650), CD107a (H4A3: BV711), CD4 (RPA-TA: BV570, BV605), CD45RO (UCHL1: BV785), CD27 (O323: BV650), CD3 (UCHT-1: Ax700), and T-bet (4B10: BV711) from Biolegend (San Diego, CA). Unlabeled CD28 (L293), and CD49d (L25) were from BD Pharmingen (San Diego, CA). Eomesodermin (WD1928: PE-eFluor610) and S1PR1 (SW4GYPP: eFluor660) were from ThermoFisher (Waltham, MA). The HIV-1 Gag peptide pool (p55, HXB2 sequence) consisted of 15-mers with an 11 amino acid overlap (BD Biosciences). *Staphylococcal* enterotoxin B (SEB) was from Sigma Aldrich.

Antigen Stimulation and Intracellular Cytokine Staining (ICS)

Surface and intracellular staining was performed as described[25] on freshly isolated blood and rectosigmoid mononuclear cells rested overnight at 37°C, 5% CO_2. For stimulation assays, cells were incubated at 2×10^6 cells per 200μL R-15 for 6h in the presence of CD28 (1μg/mL) and CD49d (1μg/mL), anti-CD107a, 1μM GolgiStop™ (BD Biosciences), brefeldin A (5μg/mL, Sigma Aldrich) and the appropriate antigens: Gag-peptide pool (3.5μg/mL), *Staphylococcal* enterotoxin B (5μg/mL), or media containing DMSO (peptide solvent) as negative control. Cells were incubated for 10 minutes in PBS with 0.5mM EDTA prior to staining for surface markers and viability (Aqua Dead cell stain kit, Invitrogen) for 20 minutes at room temperature. Cells were fixed in 4% paraformaldehyde (PFA) and permeabilized using FACS Perm 2 (BD Biosciences) prior to intracellular staining for CD3, IFN-γ, MIP-1β, TNF-α, and IL-2. The Transcription Factor Buffer Set (BD Biosciences) was substituted for 4% PFA and FACS Perm 2 when staining for transcription factors. In such cases, cells were fixed with Transcription Factor Fix/Perm Buffer for 40 minutes at 4°C, washed twice in Transcription Factor Perm/Wash Buffer, and stained with antibodies for 40 minutes at 4°C in Transcription Factor Perm/Wash. For all protocols, after staining, cells were re-suspended in 1% PFA and stored at 4°C in the dark until analysis within 24h.

Data Acquisition and Analysis

Flow cytometry data were acquired with an LSR II cytometer and FACSDiva™ software (Becton Dickinson Immuno-cytometry Systems). Analysis was performed using Flowjo software (Flowjo LLC, Ashland, OR). Fluorescence minus one (FMO) samples and known negative populations were used to aid in gating (Supplementary Figures 1a, 6b, 8). The distinction between CD103 negative, low and high populations was made visually as shown in Supplementary Figure 8. Tissue resident responses were identified using Boolean gating within the live, $CD3^+$, $CD8^+$, $CD45RO^+$, $CD103^+CD69^+S1PR1^-$ subset for T_{RM} or live, $CD3^+$, $CD8^+$, $CD45RO^-$, $CD103^+CD69^+S1PR1^-$ subset for rT_{EFF}. An in-house statistical

algorithm was used to determine whether antigen-specific responses differed significantly from the negative control[25]. For responses deemed statistically significant, net responses were then calculated by subtracting negative control values from antigen-specific responses. SPICE software was used to visualize multifunctional T-cell populations[48]. Statistical analyses were performed with GraphPad Prism V.6 (Graphpad Software, San Diego, CA) or SPICE. Non-parametric statistical tests included Wilcoxon matched-pairs signed rank test for paired samples, Mann-Whitney test for unpaired samples, Spearman correlation and linear regression analysis.

In Situ Tetramer Staining and Immunohistochemistry

Fresh biopsy specimens were shipped in complete media on ice overnight to the University of Minnesota. Biopsies were cut into 2 to 4 sections using a scalpel and stained with MHC-tetramers, CD103, and CD8 antibodies as previously described[49, 50]. Red background from MHC tetramer staining was used for morphological identification of intestinal crypts. Biotinylated MHC-class I monomers were loaded with peptides (National Institute of Health Tetramer Core Facility, Emory University, Atlanta GA) and converted to MHC-class I tetramers. HLA-B*57 molecules were loaded with HIV-1 Gag IW9 (ISPRTLNAW) or QW9 (QASQEVKNW) peptides. HLA-B*07 molecules were loaded with Nef TL10 (TPNGSIFTTL) peptides. An irrelevant peptide MART (ELAGIGILTV) from melanoma protein was used as negative control. Fresh tissue sections were incubated with MHC-class I tetramers (0.5 μg/ml), mouse-anti-human CD103 Abs (2.5 μg/ml, Biolegend), and rat-anti-human CD8 Abs (2 μg/ml, Acris). For secondary incubations, sections were incubated with rabbit-anti-FITC Abs (0.5 μg/mL, BioDesign, Saco, ME). For tertiary incubations, sections were incubated with Cy3-conjugated goat-anti-rabbit Abs (0.3 μg/mL, Jackson ImmunoResearch Laboratories), Alexa 488-conjugated goat-anti-mouse Abs (0.75 μg/mL, Molecular Probes), and Cy5-conjugated goat-anti-rat Abs (0.3 μg/mL, Jackson ImmunoResearch Laboratories). Sections stained with secondary antibodies alone were used as negative controls for CD103 and CD8 staining. Sections were imaged using an Olympus FluoView 1000 microscope. Confocal z-series were collected from ~3 μm from the surface of the section to 30–45 μm into the tissue. Montage images of multiple 800 × 800 pixels were created and used for analysis.

Quantitative Image Analysis

Anatomical compartments of rectosigmoid mucosa, crypts and intraepithelial lymphocytes were identified morphologically by increasing the red background from MHC tetramers to allow identification of goblet cells. The ~10 μm area directly adjacent was defined as the border. Surrounding areas with abundant $CD8^+$ T cells and diffuse red background were identified as lamina propria. Areas that were ambiguous in structure were not included. To determine levels of CD103 expression, $CD8^+$ T cells with no detectable CD103 staining above background were scored as CD103 negative, cells with CD103 staining 2–5× greater than background were scored as $CD103^{low}$, cells with CD103 staining 6× or greater than background were scored as $CD103^{high}$.

Supplementary Material

Refer to Web version on PubMed Central for supplementary material.

Acknowledgments

The authors thank Rebecca Hoh, Montha Pao, Monika Deswal and the clinical staff at San Francisco General Hospital for their assistance with participant recruitment and sample collection. We thank the participants for their willingness to contribute to this study. The SCOPE cohort was supported by the Delaney AIDS Research Enterprise (DARE; AI096109 and AI127966), NIAID (K24 AI069994), and the UCSF/Gladstone Institute of Virology & Immunology CFAR (P30 AI027763). We also thank Dr. Alex Khoruts, University of Minnesota, for assistance with identification of anatomical compartments in rectosigmoid tissue samples. This work was supported by NIH/NIAID R01-AI057020 to BLS. The UC Davis Flow Cytometry Shared Resource Laboratory (FCSR) was supported by grants from the National Institutes of Health: NCI P30 CA0933730, and NIH NCRR C06-RR12088, S10-RR12964, S10-RR026825 and S10-OD018223-01A1; and the James B. Pendleton Charitable Trust. We thank the FCSR staff members Ms. Bridget McLaughlin and Mr. Jonathan Van Dyke, for assistance with flow cytometry.

References

1. Hatano H, et al. Comparison of HIV DNA and RNA in gut-associated lymphoid tissue of HIV-infected controllers and noncontrollers. AIDS. 2013; 27:2255–2260. [PubMed: 24157906]
2. Shacklett BL, Ferre AL. Mucosal immunity in HIV controllers: the right place at the right time. Curr Opin HIV AIDS. 2011; 6:202–207. [PubMed: 21399497]
3. Barouch DH, Deeks SG. Immunologic strategies for HIV-1 remission and eradication. Science. 2014; 345:169–174. [PubMed: 25013067]
4. Masopust D, Picker LJ. Hidden memories: frontline memory T cells and early pathogen interception. J Immunol. 2012; 188:5811–5817. [PubMed: 22675215]
5. Shacklett BL, Anton PA. HIV Infection and Gut Mucosal Immune Function: Updates on Pathogenesis with Implications for Management and Intervention. Curr Infect Dis Rep. 2010; 12:19–27. [PubMed: 20174448]
6. Masopust D, Vezys V, Wherry EJ, Barber DL, Ahmed R. Cutting edge: gut microenvironment promotes differentiation of a unique memory CD8 T cell population. J Immunol. 2006; 176:2079–2083. [PubMed: 16455963]
7. Casey KA, et al. Antigen-independent differentiation and maintenance of effector-like resident memory T cells in tissues. J Immunol. 2012; 188:4866–4875. [PubMed: 22504644]
8. Schenkel JM, Masopust D. Tissue-resident memory T cells. Immunity. 2014; 41:886–897. [PubMed: 25526304]
9. Thome JJ, Farber DL. Emerging concepts in tissue-resident T cells: lessons from humans. Trends Immunol. 2015; 36:428–435. [PubMed: 26072286]
10. Mueller SN, Mackay LK. Tissue-resident memory T cells: local specialists in immune defence. Nat Revs Immunol. 2016; 16:79–89. [PubMed: 26688350]
11. Hofmann M, Pircher H. E-cadherin promotes accumulation of a unique memory CD8 T-cell population in murine salivary glands. Proc Natl Acad Sci U S A. 2011; 108:16741–16746. [PubMed: 21930933]
12. Mackay LK, et al. The developmental pathway for CD103(+)CD8+ tissue-resident memory T cells of skin. Nat Immunol. 2013; 14:1294–1301. [PubMed: 24162776]
13. Skon CN, et al. Transcriptional downregulation of S1pr1 is required for the establishment of resident memory CD8+ T cells. Nat Immunol. 2013; 14:1285–1293. [PubMed: 24162775]
14. Mackay LK, et al. Cutting edge: CD69 interference with sphingosine-1-phosphate receptor function regulates peripheral T cell retention. J Immunol. 2015; 194:2059–2063. [PubMed: 25624457]
15. Wakim LM, et al. The molecular signature of tissue resident memory CD8 T cells isolated from the brain. J Immunol. 2012; 189:3462–3471. [PubMed: 22922816]

16. Mackay LK, et al. T-box Transcription Factors Combine with the Cytokines TGF-beta and IL-15 to Control Tissue-Resident Memory T Cell Fate. Immunity. 2015; 43:1101–1111. [PubMed: 26682984]
17. Mackay LK, et al. Long-lived epithelial immunity by tissue-resident memory T (TRM) cells in the absence of persisting local antigen presentation. Proc Natl Acad Sci U S A. 2012; 109:7037–7042. [PubMed: 22509047]
18. Li H, et al. Durable mucosal simian immunodeficiency virus-specific effector memory T lymphocyte responses elicited by recombinant adenovirus vectors in rhesus monkeys. J Virol. 2011; 85:11007–11015. [PubMed: 21917969]
19. Carbone FR. Tissue-Resident Memory T Cells and Fixed Immune Surveillance in Nonlymphoid Organs. J Immunol. 2015; 195:17–22. [PubMed: 26092813]
20. Zhu J, et al. Immune surveillance by CD8alphaalpha+ skin-resident T cells in human herpes virus infection. Nature. 2013; 497:494–497. [PubMed: 23657257]
21. Gebhardt T, et al. Memory T cells in nonlymphoid tissue that provide enhanced local immunity during infection with herpes simplex virus. Nat Immunol. 2009; 10:524–530. [PubMed: 19305395]
22. Schenkel JM, et al. T cell memory. Resident memory CD8 T cells trigger protective innate and adaptive immune responses. Science. 2014; 346:98–101. [PubMed: 25170049]
23. Schenkel JM, Fraser KA, Vezys V, Masopust D. Sensing and alarm function of resident memory CD8(+) T cells. Nat Immunol. 2013; 14:509–513. [PubMed: 23542740]
24. Bergsbaken T, Bevan MJ. Proinflammatory microenvironments within the intestine regulate the differentiation of tissue-resident CD8(+) T cells responding to infection. Nat Immunol. 2015; 16:406–414. [PubMed: 25706747]
25. Critchfield JW, et al. Magnitude and complexity of rectal mucosa HIV-1-specific CD8+ T-cell responses during chronic infection reflect clinical status. PLoS One. 2008; 3:e3577. [PubMed: 18974782]
26. Ferre AL, et al. Mucosal immune responses to HIV-1 in elite controllers: a potential correlate of immune control. Blood. 2009; 113:3978–3989. [PubMed: 19109229]
27. Kiniry BE, et al. Predominance of weakly cytotoxic, T-betLowEomesNeg CD8+ T-cells in human gastrointestinal mucosa: implications for HIV infection. Mucosal Immunol. 2016; 10:1008–1020. [PubMed: 27827375]
28. Sathaliyawala T, et al. Distribution and compartmentalization of human circulating and tissue-resident memory T cell subsets. Immunity. 2013; 38:187–197. [PubMed: 23260195]
29. Booth JS, et al. Characterization and functional properties of gastric tissue-resident memory T cells from children, adults, and the elderly. Front Immunol. 2014; 5:294. [PubMed: 24995010]
30. Shacklett BL, et al. Trafficking of human immunodeficiency virus type 1-specific CD8+ T cells to gut-associated lymphoid tissue during chronic infection. J Virol. 2003; 77:5621–5631. [PubMed: 12719554]
31. Thome JJ, et al. Spatial map of human T cell compartmentalization and maintenance over decades of life. Cell. 2014; 159:814–828. [PubMed: 25417158]
32. Hamann D, et al. Phenotypic and functional separation of memory and effector human CD8+ T cells. J Exp Med. 1997; 186:1407–1418. [PubMed: 9348298]
33. Mackay CR. Dual personality of memory T cells. Nature. 1999; 401:659–660. [PubMed: 10537102]
34. Cepek KL, et al. Adhesion between epithelial cells and T lymphocytes mediated by E-cadherin and the alpha E beta 7 integrin. Nature. 1994; 372:190–193. [PubMed: 7969453]
35. Agace WW, Higgins JM, Sadasivan B, Brenner MB, Parker CM. T-lymphocyte-epithelial-cell interactions: integrin alpha(E)(CD103)beta(7), LEEP-CAM and chemokines. Curr Opin Cell Biol. 2000; 12:563–568. [PubMed: 10978890]
36. Sheridan BS, et al. Oral infection drives a distinct population of intestinal resident memory CD8(+) T cells with enhanced protective function. Immunity. 2014; 40:747–757. [PubMed: 24792910]
37. Burgener A, McGowan I, Klatt NR. HIV and mucosal barrier interactions: consequences for transmission and pathogenesis. Curr Opin Immunol. 2015; 36:22–30. [PubMed: 26151777]

38. Laidlaw BJ, et al. CD4+ T cell help guides formation of CD103+ lung-resident memory CD8+ T cells during influenza viral infection. Immunity. 2014; 41:633–645. [PubMed: 25308332]
39. Hansen SG, et al. Immune clearance of highly pathogenic SIV infection. Nature. 2013; 502:100–104. [PubMed: 24025770]
40. Ferre AL, et al. Immunodominant HIV-specific CD8+ T-cell responses are common to blood and gastrointestinal mucosa, and Gag-specific responses dominate in rectal mucosa of HIV controllers. J Virol. 2010; 84:10354–10365. [PubMed: 20668079]
41. Park SL, Mackay LK, Gebhardt T. Distinct recirculation potential of CD69+CD103− and CD103+ thymic memory CD8+ T cells. Immunol Cell Biol. 2016
42. Mowat AM. Anatomical basis of tolerance and immunity to intestinal antigens. Nat Revs Immunol. 2003; 3:331–341. [PubMed: 12669023]
43. Zhang N, Bevan MJ. Transforming growth factor-beta signaling controls the formation and maintenance of gut-resident memory T cells by regulating migration and retention. Immunity. 2013; 39:687–696. [PubMed: 24076049]
44. Oh SA, Li MO. TGF-beta: guardian of T cell function. J Immunol. 2013; 191:3973–3979. [PubMed: 24098055]
45. Pauken KE, Wherry EJ. Overcoming T cell exhaustion in infection and cancer. Trends Immunol. 2015; 36:265–276. [PubMed: 25797516]
46. Shacklett BL, Critchfield JW, Lemongello D. Isolating mucosal lymphocytes from biopsy tissue for cellular immunology assays. Methods Mol Biol. 2009; 485:347–356. [PubMed: 19020836]
47. Shacklett BL, et al. Optimization of methods to assess human mucosal T-cell responses to HIV infection. J Immunol Methods. 2003; 279:17–31. [PubMed: 12969544]
48. Roederer M, Nozzi JL, Nason MC. SPICE: exploration and analysis of post-cytometric complex multivariate datasets. Cytometry Part A. 2011; 79:167–174.
49. Skinner PJ, Daniels MA, Schmidt CS, Jameson SC, Haase AT. Cutting edge: In situ tetramer staining of antigen-specific T cells in tissues. J Immunol. 2000; 165:613–617. [PubMed: 10878330]
50. Skinner PJ, Haase AT. In situ staining using MHC class I tetramers. Curr Protoc Immunol. 2005; Chapter 17(Unit 17.4)

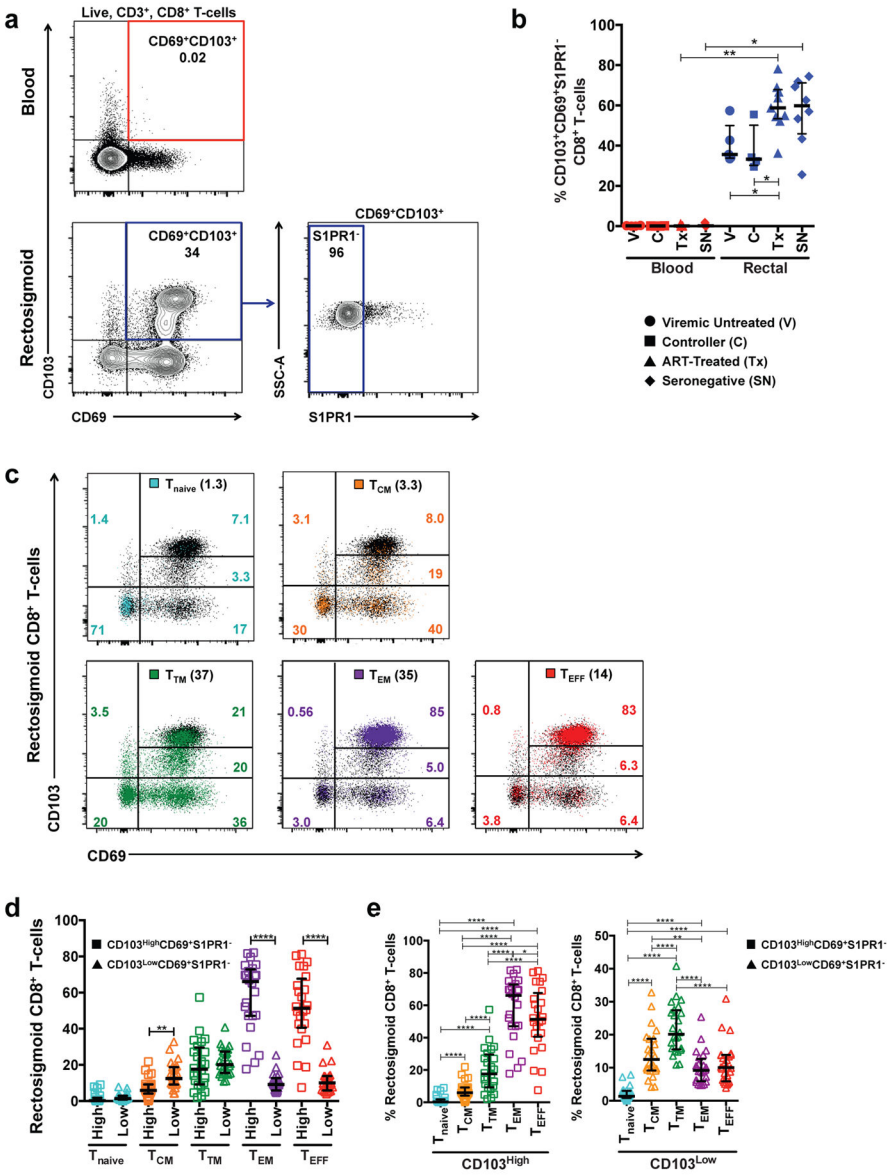

Figure 1.

Characterization and distribution of tissue-resident CD8$^+$ T-cells in the rectosigmoid mucosa of chronically HIV-1-infected and seronegative participants. **(a)** Representative flow cytometry plot displaying surface staining of tissue-resident markers and gating strategy used to identify live, CD3$^+$, tissue resident CD8$^+$ T-cells as CD103$^+$CD69$^+$S1PR1$^-$ in blood (red) and rectosigmoid mucosa (blue). **(b)** Differences in the frequency of CD103$^+$CD69$^+$S1PR1$^-$ CD8$^+$ T-cells between blood and rectosigmoid mucosa across HIV-1 disease status. **(c)** Representative flow cytometry plot demonstrating the difference in CD103 fluorescence intensity and CD69 expression in rectosigmoid naïve (T_{naive}, aqua), central memory (T_{CM}, orange), transitional memory (T_{TM}, green), effector memory (T_{EM}, purple), and effector (T_{EFF}, red) CD8$^+$ T-cells. Numbers in parentheses indicate the percentage of the memory subset in the total rectosigmoid CD8$^+$ T-cell population; colored numbers indicate frequency of the memory subset in each quadrant. Memory/effector

subsets were first identified by differential expression of CD45RO, CD27, and CCR7 as described in the text. **(d)** Comparison of the frequencies of rectosigmoid $CD103^{High}$ and $CD103^{Low}$ $CD69^{+}S1PR1^{-}$ $CD8^{+}$ T-cells within each memory subset, or **(e)** between memory subsets in a combined group of chronically HIV-1-infected and seronegative participants. Horizontal bars represent median, whiskers indicate interquartile ranges with the level of significance shown with asterisks as follows: * P <0.05, ** P <0.01, *** P <0.001, **** P <0.0001.

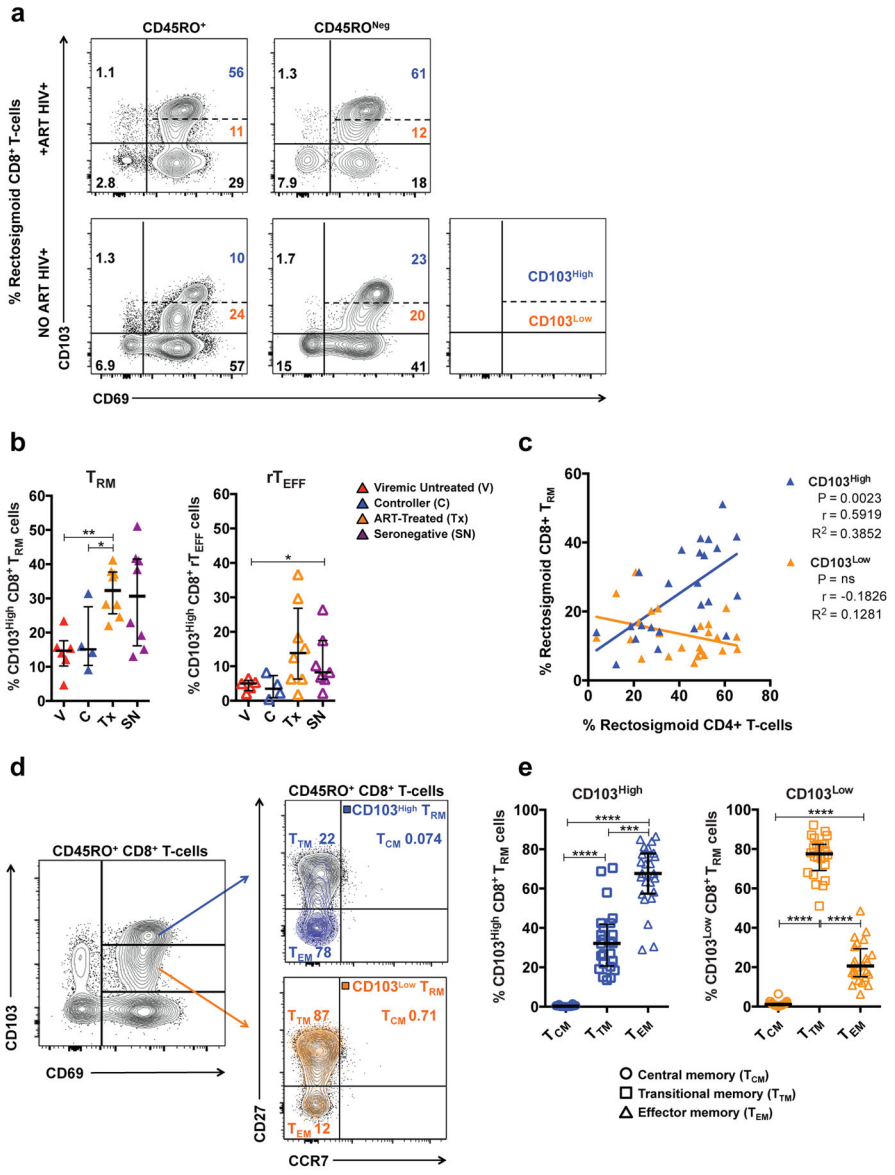

Figure 2.

Distribution, association with rectosigmoid $CD4^+$ T-cells, and maturation status of $CD103^{High}$ and $CD103^{Low}$ tissue-resident $CD8^+$ T-cells. **(a)** Representative flow cytometry plot showing differences in the proportion of $CD103^{High}$ (blue) and $CD103^{Low}$ (orange) $CD45RO^+$ and $CD45RO^{Neg}$ $CD8^+$ T-cells between a chronically HIV-1-infected individual on ART (top panel) and a chronically HIV-1-infected individual not on ART (bottom panel). **(b)** Differences in the frequency of rectosigmoid $CD103^{High}$ $CD8^+$ T_{RM} and rT_{EFF} cells across HIV-1-disease status. **(c)** Association between the frequency of rectosigmoid $CD4^+$ T-cells and the frequency of rectosigmoid $CD103^{High}$ and $CD103^{Low}$ T_{RM} $CD8^+$ T-cells in all study participants. **(d)** Representative flow cytometry plot showing differences in the expression of memory markers CD27 and CCR7 between $CD103^{High}$ and $CD103^{Low}$ rectosigmoid $CD8^+$ T_{RM} cells. **(e)** Distribution of central memory (T_{CM}), transitional memory (T_{TM}), and effector memory (T_{EM}) subsets within $CD103^{High}$ and $CD103^{Low}$

rectosigmoid $CD8^+$ T_{RM} in a combined group of all study participants. Associations calculated using non-parametric Spearman correlation and linear regression analyses. Horizontal bars represent median, whiskers indicate interquartile range with the level of significance indicated with asterisks as follows: * P <0.05, ** P <0.01, *** P <0.001, **** P <0.0001.

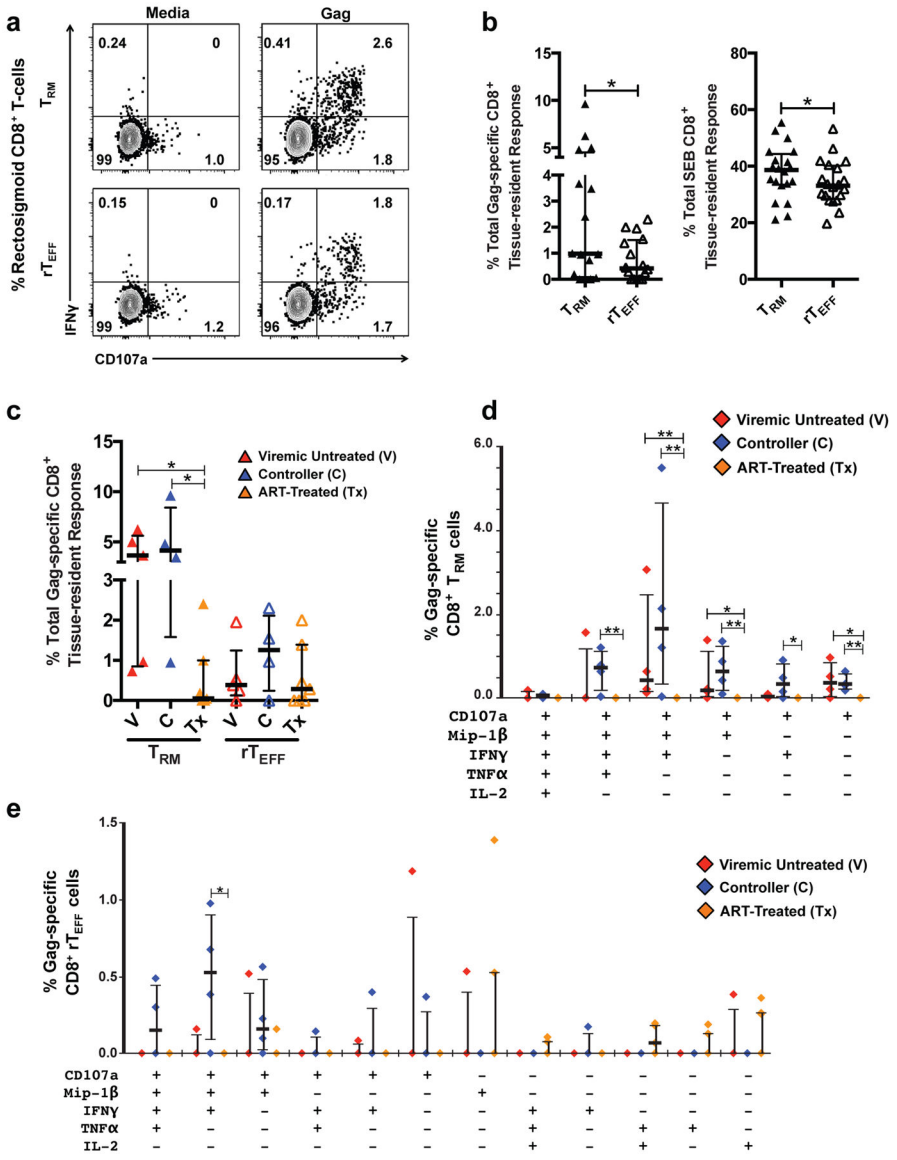

Figure 3.

Responses of rectosigmoid CD8$^+$ T_{RM} cells to antigenic stimulation. **(a)** Representative flow cytometry plot demonstrating degranulation (CD107a) and IFN-γ-production following stimulation with an HIV-1 Gag-peptide pool or medium containing DMSO (negative control) by rectosigmoid CD8$^+$ T_{RM} (top) and rT_{EFF} (bottom) from an HIV-1$^+$ controller. **(b)** Difference in the frequency of CD8$^+$ T_{RM} and rT_{EFF} cells responding to Gag-peptide and SEB stimulation. **(c)** Total percentage of rectosigmoid CD8+ T_{RM} and rT_{EFF} responding in any way (TNF-α, IFN-γ, IL-2, CD107a, and/or MIP-1β) to HIV-1 Gag stimulation. For each subject, the total HIV-1 Gag-specific response shown in (c) was calculated by combining all non-overlapping Boolean categories that are displayed individually in panels (d), for T_{RM}, and (e), or rT_{EFF}. **(d)** Difference in percentages of poly- and monofunctional Gag-specific rectosigmoid CD8$^+$ T_{RM} cells across HIV-1 disease status. **(e)** Difference in percentages of poly-and monofunctional Gag-specific rectosigmoid CD8$^+$ rT_{EFF} cells across

HIV disease status. Response data were analyzed using Boolean gating of responding populations within live, $CD3^+$, $CD8^+$, $CD45RO^+$ or $CD45RO^{Neg}$, $CD103^+CD69^+S1PR1^-$ gates. Co-expression analyses were generated using SPICE software. Poly- and monofunctional combinations with negligible responses were omitted. Horizontal bars represent medians, whiskers indicate interquartile ranges with the level of significance shown with asterisks as follows: * P <0.05, ** P <0.01, *** P <0.001, **** P <0.0001.

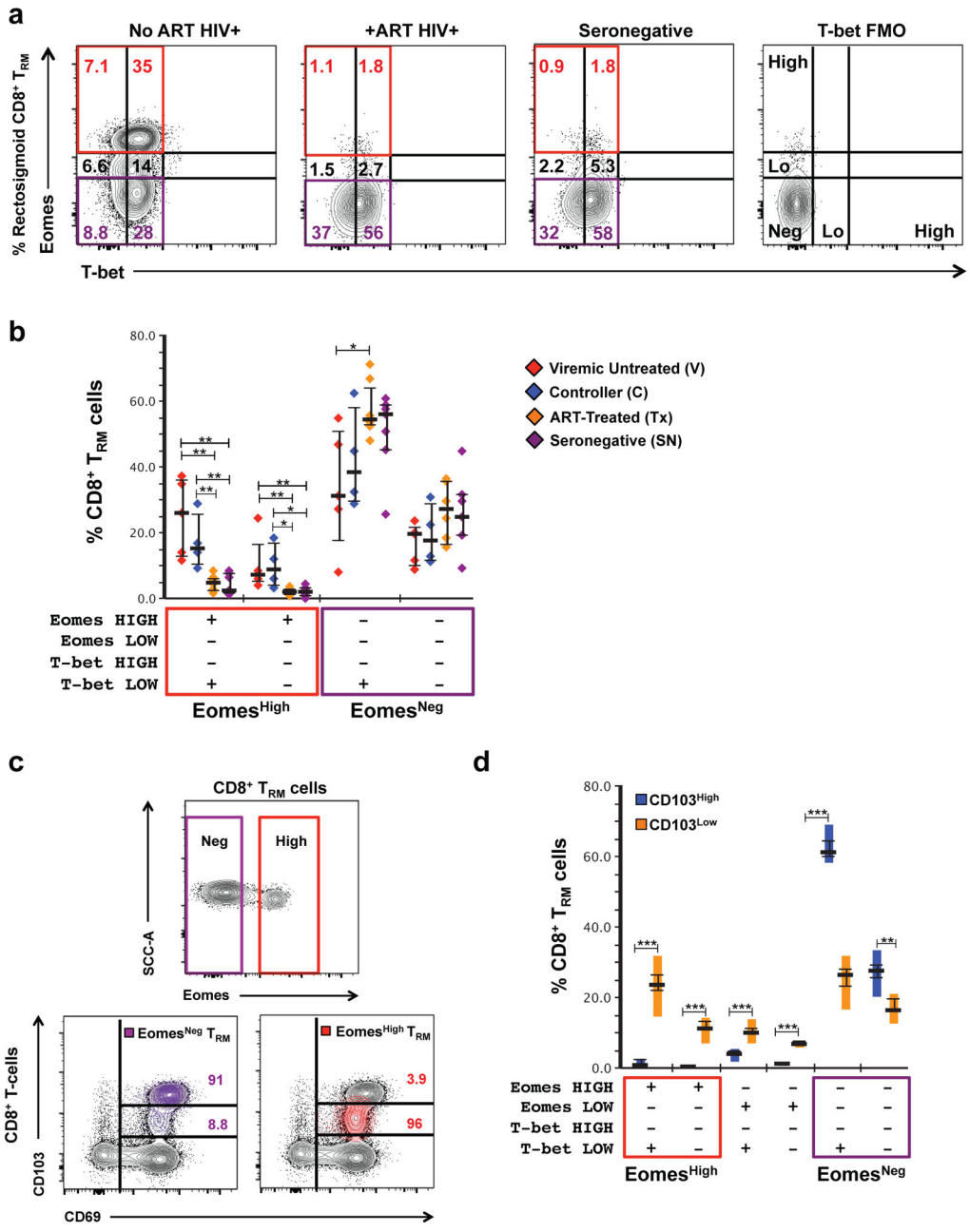

Figure 4.

Expression of T-bet and Eomesodermin in tissue-resident CD8$^+$ T-cells varies with HIV-1-disease status and CD103 fluorescence intensity. **(a)** Representative flow cytometry plot displaying differences in expression of T-bet and Eomesodermin (Eomes) in rectosigmoid CD8$^+$ T_{RM} between a chronically HIV-1-infected participant not on ART (far left), a chronically HIV-1-infected participant on ART (second from left), and a seronegative participant (second from right). T-bet FMO control is displayed for comparison (far right). **(b)** Differences in the frequency of Eomes^{High} and Eomes^{Neg} rectosigmoid CD8$^+$ T_{RM} across HIV-1-disease status. Horizontal bars represent medians, whiskers represent

interquartile ranges. **(c)** Representative flow cytometry plot displaying differences in CD103 fluorescence intensity between $Eomes^{High}$ and $Eomes^{Neg}$ rectosigmoid $CD8^+$ T_{RM}. **(d)** Difference in Eomes expression between $CD103^{High}$ and $CD103^{Low}$ rectosigmoid $CD8^+$ T_{RM} cells in a combined group of all study participants. Vertical bars represent interquartile ranges, horizontal bars represent medians, whiskers represent standard error of the mean. Co-expression analysis was generated using SPICE software. Level of significance is indicated with asterisks as follows: * P <0.05, ** P <0.01, *** P <0.001, **** P <0.0001.

Table 1

Participant Characteristics

	Gender	Race	Plasma viral load, RNA copies/mL * [Median] [Range]	CD4 count, Cells/mm^3 [Median] [Range]	Time Post HIV+ Diagnosis, years [Median] [Range]	Age, Years [Median] [Range]
Controllers (n = 4)	M, 2 F, 1 T **, 1	AA, 3 C, 1	943 <40 – 1,497	769 431 – 1,128	14 7 – 31	59 50 – 63
Viremic Untreated (n = 6)	M, 6	AA, 4 C, 2	57,995 9,436 – 308,383	324 198 – 516	14 3 – 31	48 33 – 54
ART-Treated (n = 8)	M, 6 F, 2	AA, 4 C, 4	<40 NA	770 564 – 2,658	9 6 – 30	48 28 – 67
Seronegatives (n = 8)	M, 7 F, 1	AA, 5 C, 3	NA NA	764 406 – 2,269	NA NA	49 26 – 60

M, Male; F, Female; T, Transgender;

** male-to-female.

AA, African American; C, Caucasian; NA, Not applicable.

* Median determined using only detectable viral load data points.